Carbohydrate Polymers xxx (2012) xxx–xxx

Contents lists available at SciVerse ScienceDirect

Carbohydrate Polymers

journal homepage: www.elsevier.com/locate/carbpol

Kinetics and mechanism of thermal degradation of pentose- and hexose-based carbohydrate polymers

Jamshed Akbar[a], Mohammad S. Iqbal[b,*], Shazma Massey[b,c], Rashid Masih[b]

[a] Department of Chemistry, University of Sargodha, Sargodha 40100, Pakistan
[b] Department of Chemistry, Forman Christian College, Lahore 54600, Pakistan
[c] Department of Chemistry, GC University, Lahore 54000, Pakistan

ARTICLE INFO

Article history:
Received 9 June 2012
Received in revised form 28 June 2012
Accepted 2 July 2012
Available online xxx

Keywords:
Thermogravimetry
Isoconversional analysis
Thermal degradation
Polysaccharides
Kinetic triplet
Thermal stability
Master plots

ABSTRACT

This work aims at study of thermal degradation kinetics and mechanism of pentose- and hexose-based carbohydrate polymers isolated from *Plantago ovata* (PO), *Salvia aegyptiaca* (SA) and *Ocimum basilicum* (OB). The analysis was performed by isoconversional method. The materials exhibited mainly two-stage degradation. The weight loss at ambient–115 °C characterized by low activation energy corresponds to loss of moisture. The kinetic triplets consisting of E, A and $g(\alpha)$ model of the materials were determined. The major degradation stage represents a loss of high boiling volatile components. This stage is exothermic in nature. Above 340 °C complete degradation takes place leaving a residue of 10–15%. The master plots of $g(\alpha)$ function clearly differentiated the degradation mechanism of hexose-based OB and SA polymers and pentose-based PO polymer. The pentose-based carbohydrate polymer showed D_4 type and the hexose-based polymers showed A_4 type degradation mechanism.

1. Introduction

Several plants are a renewable source of gums and mucilages which can be used in a number of applications. Some of these materials are polysaccharides having large capacity to absorb water and behave like hydrogels. *Plantago ovata*, *Ocimum basilicum*, *Salvia aegyptiaca* are among the plants which contain swellable polysaccharides which can be developed for use as thickeners, drug carriers and in tissue engineering (Akbar, Iqbal, Chaudhary, Yasin, & Massey, 2012; Barbucci, 2009; Fariba & Ebrahim, 2009; Gupta, Vermani, & Garg, 2002; Hoare & Kohane, 2008; Iqbal, Akbar, Hussain, Saghir, & Sher, 2011; Ruel-Gariépy & Leroux, 2006). In order to develop these materials for any of such applications there is a need to study their thermal stability and degradation pattern. By use of thermal analysis techniques including thermogravimetric analysis (TGA) and differential scanning calorimetry (DSC) we can determine various thermal and kinetic parameters including thermal stability (lifetime), glass transition temperature, energy of activation (E) and degradation mechanism. These parameters are extremely helpful in knowing and predicting the thermal behavior of polymeric materials to be used for a specific application (Aggarwal, Dollimore, & Heon, 1997; Chrissafis, 2009; Iqbal, Akbar, Saghir, et al., 2011; Villetti et al., 2002; Yang, Yan, Chen, Lee, & Zheng, 2007; Zohuriaan & Shokrolahi, 2004).

There are different methods available to analyze and interpret the thermal analysis data. These are single heating rate model-fitting methods (e.g., Broido, Coats–Redfern, Horowitz–Metzger methods, etc.) and multiple heating rate model-free methods (also known as isoconversional methods). The single heating rate methods are generally criticized for giving unreliable estimates of thermal parameters. The multiple heating rate methods provide good estimates of activation energy (Vyazovkin et al., 2011).

The polymers from *O. basilicum* (OB), *S. aegyptiaca* (SA) and *P. ovata* (PO) were included in this study because they have well-defined chemical composition and are being widely used as thickeners for food and pharmaceutical products (Chatterjee & Mukherjee, 1958; Hosseini-Parvar, Matia-Merino, Goh, Razavi, & Mortazavi, 2010; Saghir, Iqbal, Hussain, Koschella, & Heinze, 2008; Singh, 2007). Very little information is available on thermal degradation behavior of these materials. We recently reported a study using the single-heating-rate method (Iqbal, Akbar, Saghir, et al., 2011). No detailed study has been carried out to determine the kinetics and mechanism of thermal degradation of these materials. In the present paper a detailed analysis of thermal data by use of isoconversional method is being reported.

* Corresponding author. Tel.: +92 300 4262813.
E-mail address: saeediq50@hotmail.com (M.S. Iqbal).

0144-8617/$ – see front matter © 2012 Elsevier Ltd. All rights reserved.
http://dx.doi.org/10.1016/j.carbpol.2012.07.008

2. Materials and methods

2.1. Materials

Seeds of SA, OB and PO were obtained from the local market and acetone was procured from E. Merck, Germany. The chemicals were used without further purification. Double-distilled water was used in the study.

2.2. Extraction of polymers from seeds

A hot-water extract of PO seeds was obtained as per reported method (Iqbal, Akbar, Hussain, et al., 2011). Briefly, the washed seeds (15 g) were heated gently to boiling in water (500 cm^3) to produce a thick solution. The seeds were filtered off and the hot-water extract was cooled, treated with acetone (about two volumes) to coagulate the polymer, separated by filtration through muslin cloth, washed with acetone and air-dried to a moisture content of 8–12% (w/w). The polymers from SA and OB seeds were obtained by using acetone as reported earlier (Iqbal, Akbar, Saghir, et al., 2011). Briefly, the seeds (15 g) were soaked in water (500 cm^3) for 6 h. The mixture was blended with blunt blades vigorously using kitchen blender. The seeds were filtered off and the thick solution was treated with acetone (about two volumes) to coagulate the gel and processed as for PO. The isolated polymers were powdered by using kitchen grinder.

2.3. Thermal analysis

The powdered polymers were subjected to a simultaneous TGA and DSC analysis by thermal analyzer SDT, Q-600 (TA instruments, USA). The thermal data were obtained at four heating rates: 5, 10, 15 and 20 °C min^{-1} in the temperature range ambient to 600 °C under nitrogen atmosphere (at 100 cm^3 min^{-1}). The baseline correction was applied to DSC scans. The data were processed by use of Universal Analysis 2000 software, version 4.2E (TA Instruments, USA), and MS Excel® 2007.

2.4. Thermal degradation kinetics

The isoconversional principle assumes that the reaction rate only depends upon the temperature at any given degree of conversion and it is independent of the reaction mechanism. This assumption provided the basis for the development of model-free methods to analyze thermal data. The integral model-free kinetic equation obtained by an approximation can be given in its more general form as Eq. (1) (Vyazovkin et al., 2011).

$$\ln \frac{\beta}{T^x} = \text{const} - y\frac{E}{RT} \quad (1)$$

where x and y are parameters determined by the type of approximation used in a particular integral isoconversional method.

The most widely used integral isoconversional method was developed by Ozawa, and Flynn and Wall in which the x and y were 0 and 1.052, respectively. However, it has been shown that with $x = 2$ and $y = 1$ in Eq. (1), more reliable estimates of E can be obtained. This result in the so-called Kissinger–Akahira–Sunose (KAS) equation (Eq. (2)) (Vyazovkin et al., 2011).

$$\ln \frac{\beta}{T^2} = \text{const} - \frac{E}{RT} \quad (2)$$

where β is the heating rate; R the general gas constant; E and T are the activation energy and temperature at a degree of conversion α. The α is defined as $(w_o - w_t)/(w_o - w_f)$, where w_t is the weight of the sample at any temperature t, w_o the initial weight and w_f the final weight at the temperature at which the mass loss is almost negligible. In the KAS method, data obtained at multiple heating rates is used and a plot of log (β/T^2) vs $1/T$ at a given α gives a straight line. From the slope of the lines E values were determined and average was reported.

It is not possible to determine A and the reaction model $(g(\alpha))$ directly from the isoconversional methods, therefore, master-plot method (Janković, 2008) was employed. Eq. (3) was used for determination of these parameters.

$$g(\alpha) = \frac{A}{\beta}\int_{T_o}^{T\alpha} \exp\left(\frac{-E}{RT}\right) dT = \frac{AE}{\beta R}\int_{x}^{\infty} \frac{\exp(-x)}{x^2} dx = \frac{AE}{\beta R}p(x) \quad (3)$$

where $x = E/RT$. At a reference point ($\alpha = 0.5$), the above equation can be re-written as Eq. (4).

$$g(0.5) = \frac{AE}{\beta R}p(x_{0.5}) \quad (4)$$

By dividing Eqs. (3) with (4) we get Eq. (5) which was used for calculation of $g(\alpha)$.

$$\frac{g(\alpha)}{g(0.5)} = \frac{p(\alpha)}{p(x_{0.5})} \quad (5)$$

The theoretical master plots were obtained by plotting $g(\alpha)/g(0.5)$ against α for various $g(\alpha)$ functions (Table 1) as reported in the literature (Turmanova, Genieva, Dimitrova, & Vlaev, 2008). The experimental master plots were constructed by plotting $p(x)/p(x_{0.5})$ against α, The integral $p(x)$ has no analytical solution but can be solved by various approximations and in this study we used Senum–Yang fourth degree approximation (Senum & Yang, 1977). The experimental α–T profile and E are required to determine $p(x)/p(x_{0.5})$, which were obtained from KAS analysis. The $g(\alpha)$ model provided best matches between experimental and theoretical master plots and was, therefore, considered as the most probable mechanism. The experimental master plots showed negligible variations at different heating rates indicating a dependence of $g(\alpha)$ only on α. A plot of the selected $g(\alpha)$ against $(E/\beta R)p(x)$ would permit the evaluation of A according to Eq. (3). The $g(\alpha)$ model was reconstructed by using E and A values obtained above in order to verify the fitness of data. These results can be extremely useful in determining the storage and service conditions for these materials in various applications. The model-free approach uses Eq. (6) to predict the lifetimes of different materials (Vyazovkin et al., 2011).

$$t_\alpha = \frac{\int_o^{T\alpha} \exp(-E\alpha/RT)dT}{\beta \exp(-E\alpha/RT_o)} \quad (6)$$

The integral in the numerator of this equation was solved by Senum–Yang fourth degree approximation.

3. Results and discussion

The isolated materials were lightweight and soft free-flowing powders having white to off-white color. The results of thermal analysis are discussed in the following sections.

3.1. Thermal degradation kinetics of PO polymer

The PO polymer is a pentose-based arabinoxylan (Fischer et al., 2004; Saghir et al., 2008). Its TGA (Fig. 1a) exhibited decomposition in four stages at ambient to 115 °C, 215–310 °C, 280–330 °C and >330 °C. The stage I (ambient to 115 °C, weight loss ≈10%) corresponds to a loss of moisture with an average E 51.58 kJ mol^{-1} (Prado & Vyazovkin, 2011). The value of E was almost constant in the range $\alpha \geq 0.25$ to $\alpha \leq 0.85$ suggesting that similar type of water is contained by the material (Fig. 2a). At stage II (215–310 °C, weight loss ≈12%) the average E was 118.15 kJ mol^{-1}. This stage marks the onset of polymer degradation. The rate vs temperature curves of the

Table 1
Various models used to describe solid state kinetics.

No.	Code	Name of the function	$g(\alpha)$ model	Rate-determining mechanism
Chemical process mechanisms				
1.	$F_{1/3}$	One-third order	$1-(1-\alpha)^{2/3}$	Chemical reaction
2.	$F_{3/4}$	Three-quarter order	$1-(1-\alpha)^{1/4}$	Chemical reaction
3.	$F_{3/2}$	One and a half order	$(1-\alpha)^{-1/2}-1$	Chemical reaction
4.	F_2	Second order	$(1-\alpha)^{-1}-1$	Chemical reaction
5.	F_3	Third order	$(1-\alpha)^{-2}-1$	Chemical reaction
Acceleratory rate equations				
6.	$P_{3/2}$	Mampel power law	$\alpha^{3/2}$	Nucleation
7.	$P_{1/2}$	Mampel power law	$\alpha^{1/2}$	Nucleation
8.	$P_{1/3}$	Mampel power law	$\alpha^{1/3}$	Nucleation
9.	$P_{1/4}$	Mampel power law	$\alpha^{1/4}$	Nucleation
Sigmoidal rate equations/Random nucleation and subsequent growth				
10.	A_1, F_1	Avrami–Erofeev equation	$-\ln(1-\alpha)$	Assumed random nucleation and its growth, $n=1$
11.	$A_{3/2}$	Avrami–Erofeev equation	$[-\ln(1-\alpha)]^{2/3}$	Assumed random nucleation and its growth, $n=1.5$
12.	A_2	Avrami–Erofeev equation	$[-\ln(1-\alpha)]^{1/2}$	Assumed random nucleation and its growth, $n=2$
13.	A_3	Avrami–Erofeev equation	$[-\ln(1-\alpha)]^{1/3}$	Assumed random nucleation and its growth, $n=3$
14.	A_4	Avrami–Erofeev equation	$[-\ln(1-\alpha)]^{1/4}$	Assumed random nucleation and its growth, $n=4$
15.	A_u	Prout–Tomkins equation	$\ln[\alpha/(1-\alpha)]$	Branching nuclei
Deceleratory rate equations/Phase boundary equations				
16.	R_1, F_0, P_1	Power law	α	Contracting disk
17.	R_2, $F_{1/2}$	Power law	$1-(1-\alpha)^{1/2}$	Contracting cylinder
18.	R_3, $F_{2/3}$	Power law	$1-(1-\alpha)^{1/3}$	Contracting sphere
Diffusion mechanism equations				
19.	D_1	Parabola equation	α^2	One-dimensional diffusion
20.	D_2	Valensi equation	$\alpha+(1-\alpha)\ln(1-\alpha)$	Two-dimensional diffusion
21.	D_3	Jander equation	$[1-(1-\alpha)^{1/3}]^2$	Three-dimensional diffusion, spherical symmetry
22.	D_4	Ginstling–Brounstein equation	$1-2\alpha/3-(1-\alpha)^{2/3}$	Three-dimensional diffusion, cylindrical symmetry
23.	D_5	Zhuravlev, Lesokin, Tempelman equation	$[(1-\alpha)^{-1/3}-1]^2$	Three-dimensional diffusion
24.	D_6	Anti-Jander equation	$[(1+\alpha)^{1/3}-1]^2$	Three-dimensional diffusion
25.	D_7	Anti-Ginstling–Brounstein equation	$1+2\alpha/3-(1+\alpha)^{2/3}$	Three-dimensional diffusion
26.	D_8	Anti-Zhuravlev, Lesokin, Tempelman equation	$[(1+\alpha)^{-1/3}-1]^2$	Three-dimensional diffusion

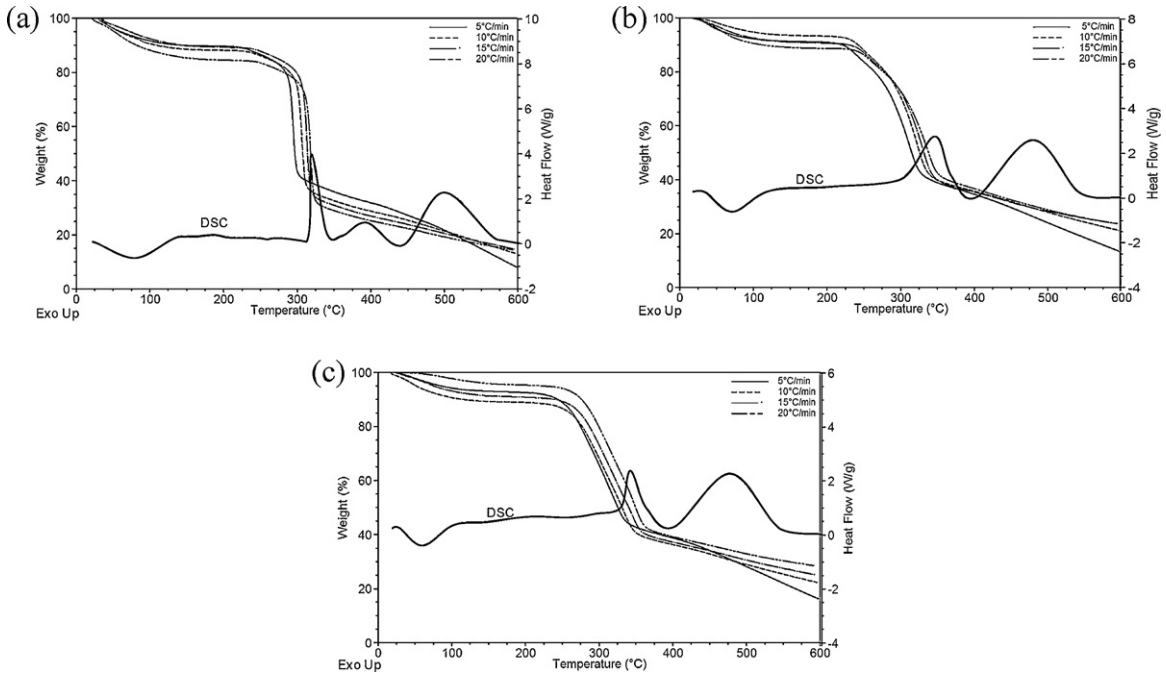

Fig. 1. TGA and DSC curves for polymers at different heating rates: (a) PO, (b) SA, (c) OB.

polymer did not show significant variation with different heating rates, which suggests a similar relationship of α with T. The master plot method (Fig. 3) suggested that this stage followed the acceleratory Maple power law model $P_{3/2}$. During this stage the value of E varies slightly (Fig. 2a) indicating occurrence of multiple reactions possibly due to merging of this stage with III. This phenomenon is well explained by acceleratory nature of $P_{3/2}$ model. The kinetic triplet determined for this stage was: $g(\alpha)=P_{3/2}$, $E=118.15\ \text{kJ mol}^{-1}$ and $A=2.89\times10^{10}\ \text{min}^{-1}$ ($\ln A=24.09$).

The major degradation of this polymer took place at stage III (280–330 °C, weight loss ≈40%). The average E for this stage was $157.78\ \text{kJ mol}^{-1}$, which was higher than that for the stage II. The E

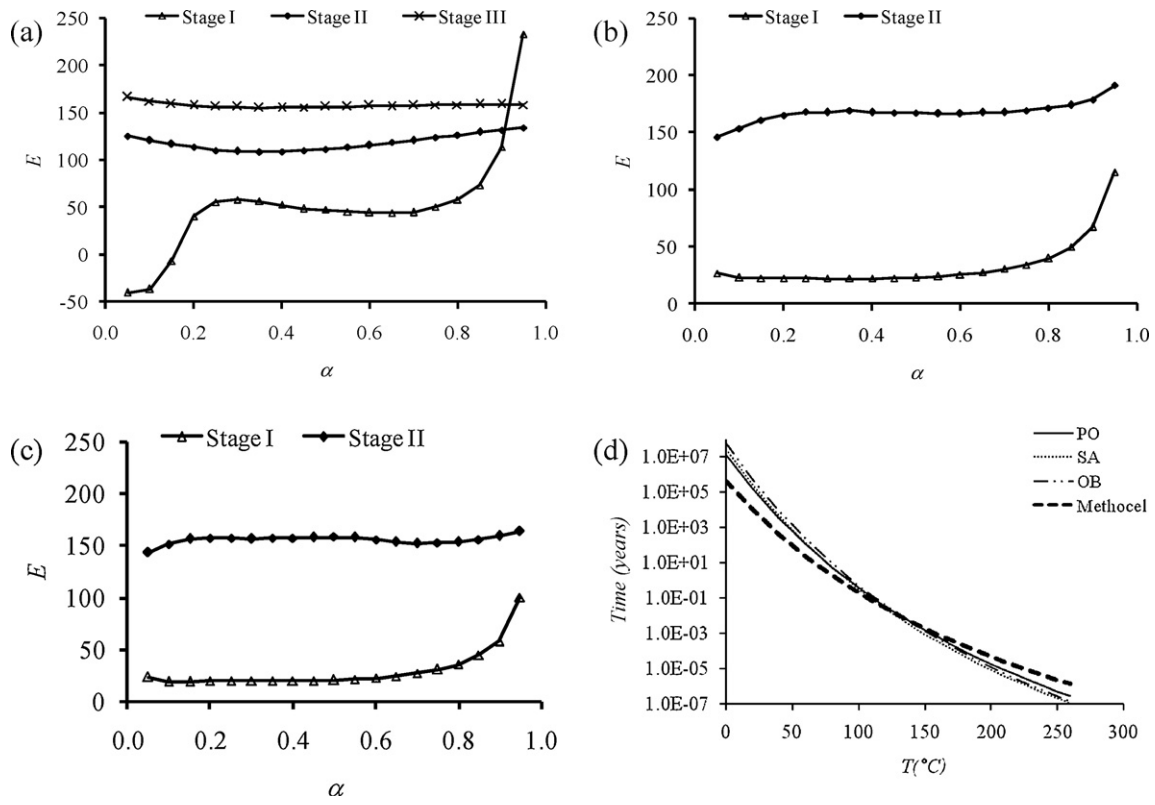

Fig. 2. (i) Variation of activation energy (E) with degree of dissociation (α) for different stages of polymers: (a) PO, (b) SA, (c) OB; and (ii) life-time prediction of polymers.

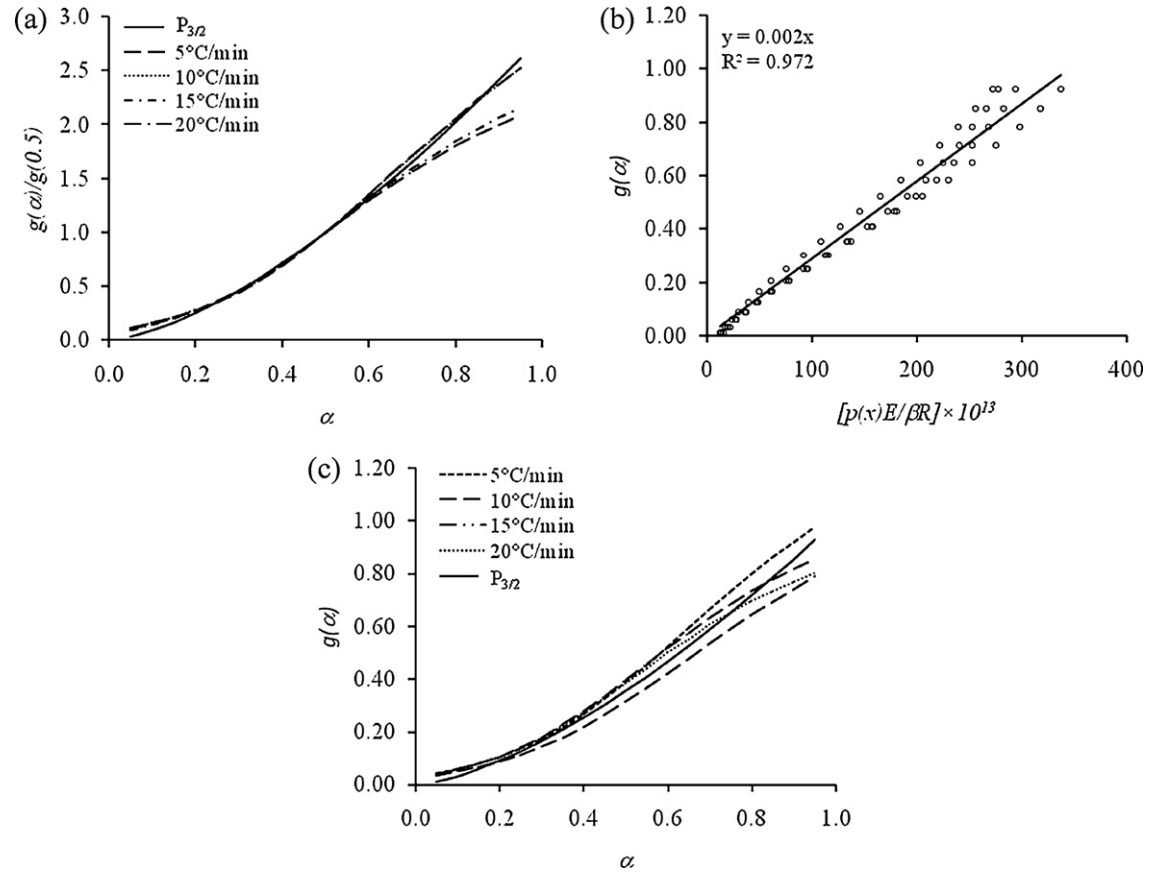

Fig. 3. Determination of kinetic model for PO degradation at stage II: (a) experimental and theoretical master plots, (b) determination of A, (c) reconstructed $g(\alpha)$ model.

Please cite this article in press as: Akbar, J., et al. Kinetics and mechanism of thermal degradation of pentose- and hexose-based carbohydrate polymers. *Carbohydrate Polymers* (2012), http://dx.doi.org/10.1016/j.carbpol.2012.07.008

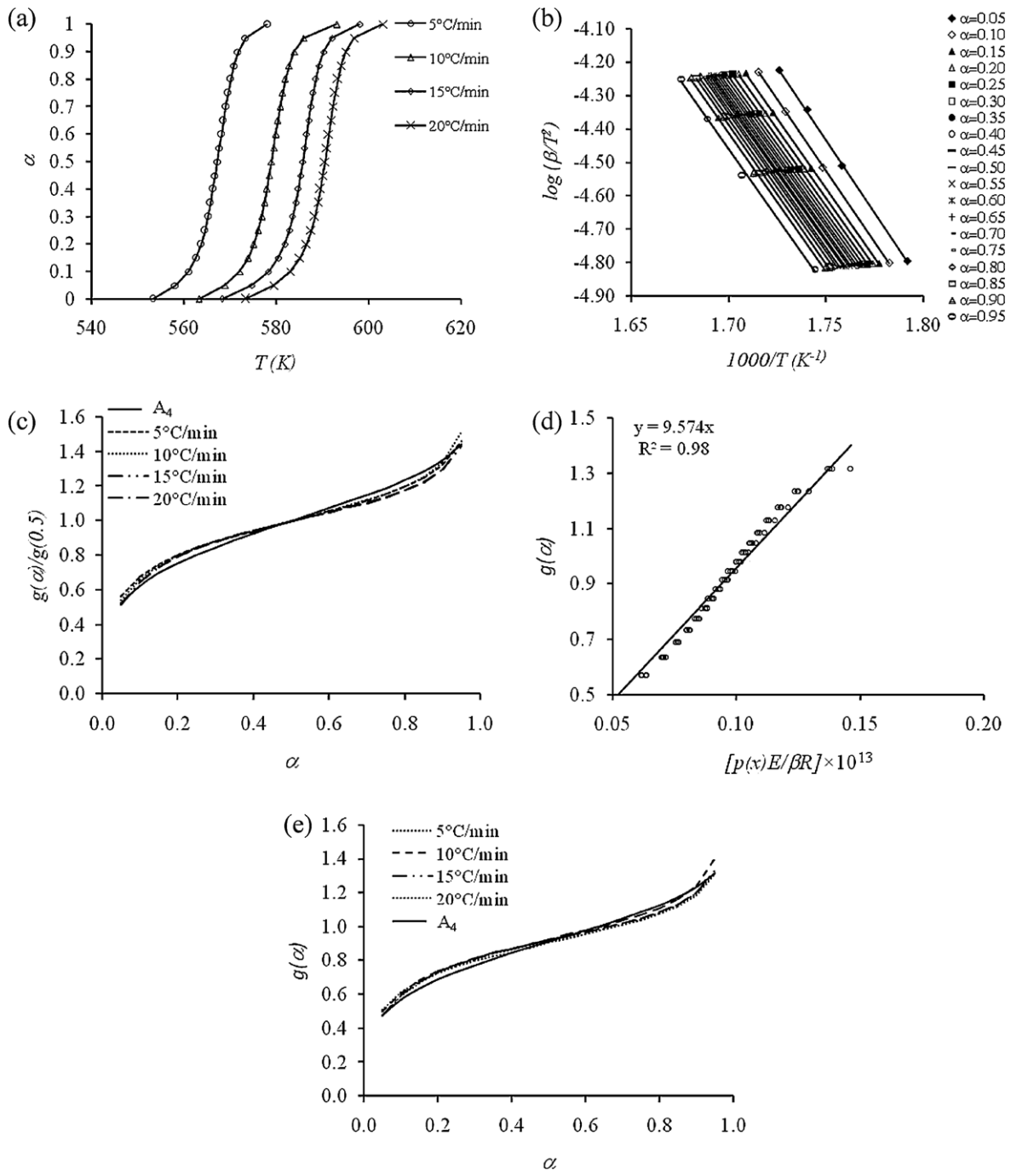

Fig. 4. Determination of kinetic model for PO degradation at stage III: (a) α–T curve, (b) KAS plot to calculate the activation energy, (c) experimental and theoretical master plots, (d) determination of A, (e) reconstructed $g(\alpha)$ model.

for this stage showed negligible variation with α (Fig. 2a) suggesting it to be a single step decomposition. The master plot method (Fig. 4) suggested that Avrami–Erofeev sigmoidal kinetic model A_4 (with $n = 4$) best describes the degradation at this stage. The A_4 is a thermal nucleation and growth model which suggests that the process is initiated by the formation of multiple nuclei in the material which subsequently grow in size leading to degradation of the polymer. The kinetic triplet for this stage was: $g(\alpha) = A_4$, $E = 157.78$ kJ mol^{-1} and $A = 9.57 \times 10^{13}$ min^{-1} ($\ln A = 32.19$). Previously the *PO* polymer (arabinoxylan) has been shown to be composed of two polysaccharide fractions with different molar mass distributions (Iqbal, Akbar, Hussain, et al., 2011; Laidlaw & Purcival, 1949, 1950), therefore, it may be suggested that at stage II the lower molar mass fraction was decomposed first followed by decomposition of the higher molar mass fraction at stage III. This was verified by treating stages II and III as the single stage, which resulted in a sigmoidal kinetics with enhanced variation in E at different α values.

The DSC scan (Fig. 1a) showed a small endotherm at stage I due to desorption of moisture. The stages II and III were associated with exothermic enthalpy changes indicating chain scission reactions resulting in a significant weight loss (total ≈52%). At the stage IV (>330 °C), the polymer is totally decomposed exothermally to gaseous products resulting in a carbon rich residue (char yield 15% at 600 °C).

For the prediction of lifetime of the polymer, stage II was used where the real degradation starts. At stage I only moisture is lost

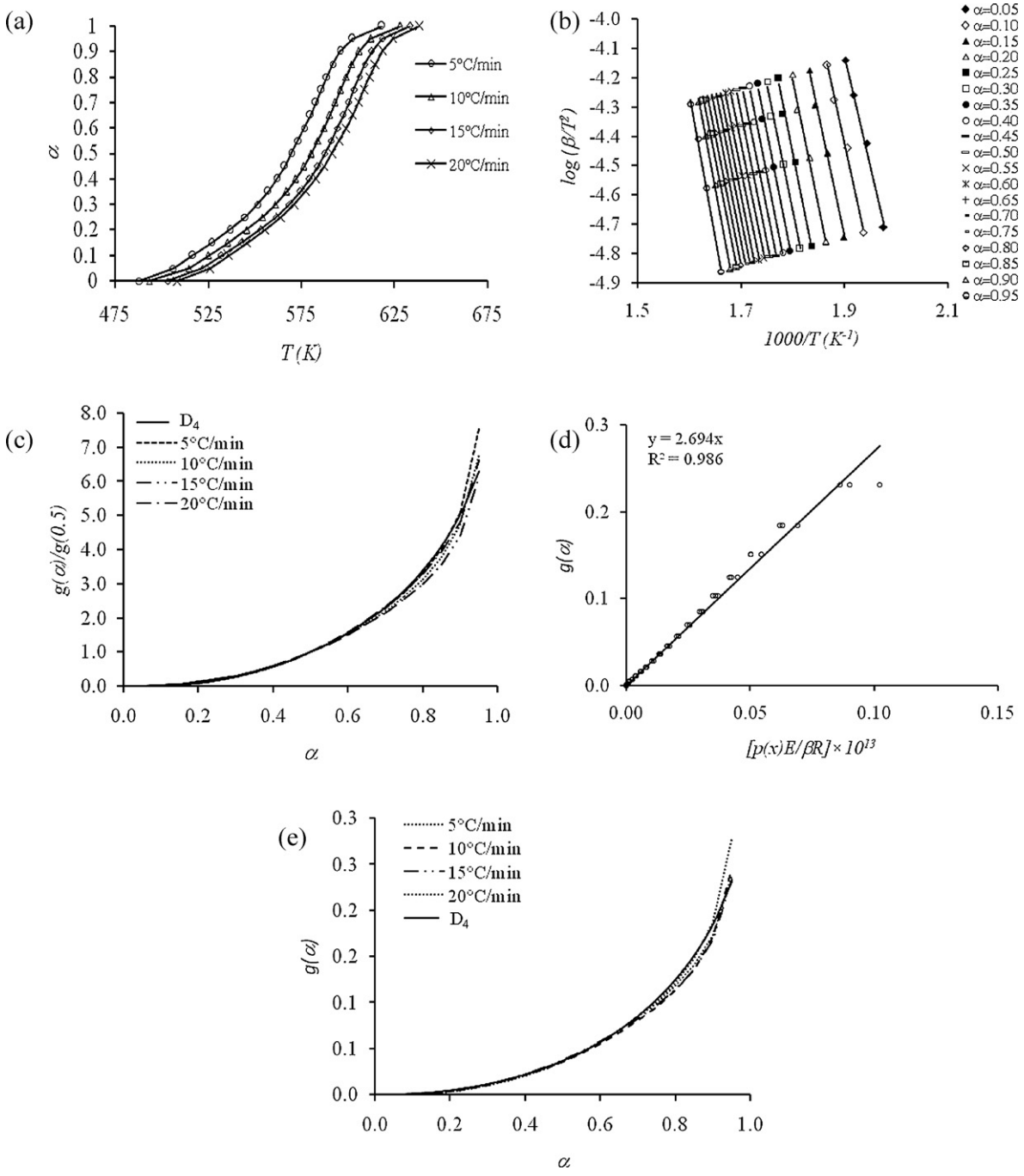

Fig. 5. Determination of kinetic model for SA degradation at stage II: (a) α–T curve, (b) KAS plot to calculate the activation energy, (c) experimental and theoretical master plots, (d) determination of A, (e) reconstructed $g(\alpha)$ model.

which may be reabsorbed by the polymer when exposed to humid environment. The lifetimes at different temperatures and 5% degree of conversion are presented in (Fig. 2d). The PO polymer appears to posses high *IPDT* (282.9 °C) and *ITS* (0.45) values comparable to those of hydroxyethyl cellulose, carboxymethyl cellulose, tragacanth gum, etc., which are commercial materials (Zohuriaan & Shokrolahi, 2004).

3.2. Thermal degradation kinetics of SA and OB polymers

The SA and OB polymers showed similar thermal decomposition behavior (Fig. 1b and c), therefore, these are discussed together in this section. They exhibited three distinct stages of weight loss occurring at ambient to 115 °C (stage I, weight loss ≈8%), 215–365 °C (stage II, weight loss ≈50%) and >365 °C (stage III). The stage I with low E value corresponds to desorption of moisture. The activation energies of the polymers at this stage were 29.11 kJ mol^{-1} (SA) and 29.65 kJ mol^{-1} (OB). Relatively lower E values than that of the PO polymer may be possibly due to weaker hydrogen bonding of water with the surfaces in these polymers.

The major degradation of these polymers occurred at stage II with average E values: 167.41 kJ mol^{-1} (SA) and 155.47 kJ mol^{-1} (OB). The decompositions at this stage followed Ginstling–Brounstein diffusion mechanism D_4 for the two polymers (Figs. 5 and 6). The corresponding A values are given in Table 2. Relatively higher *IPDT* and *ITS* values were observed for these

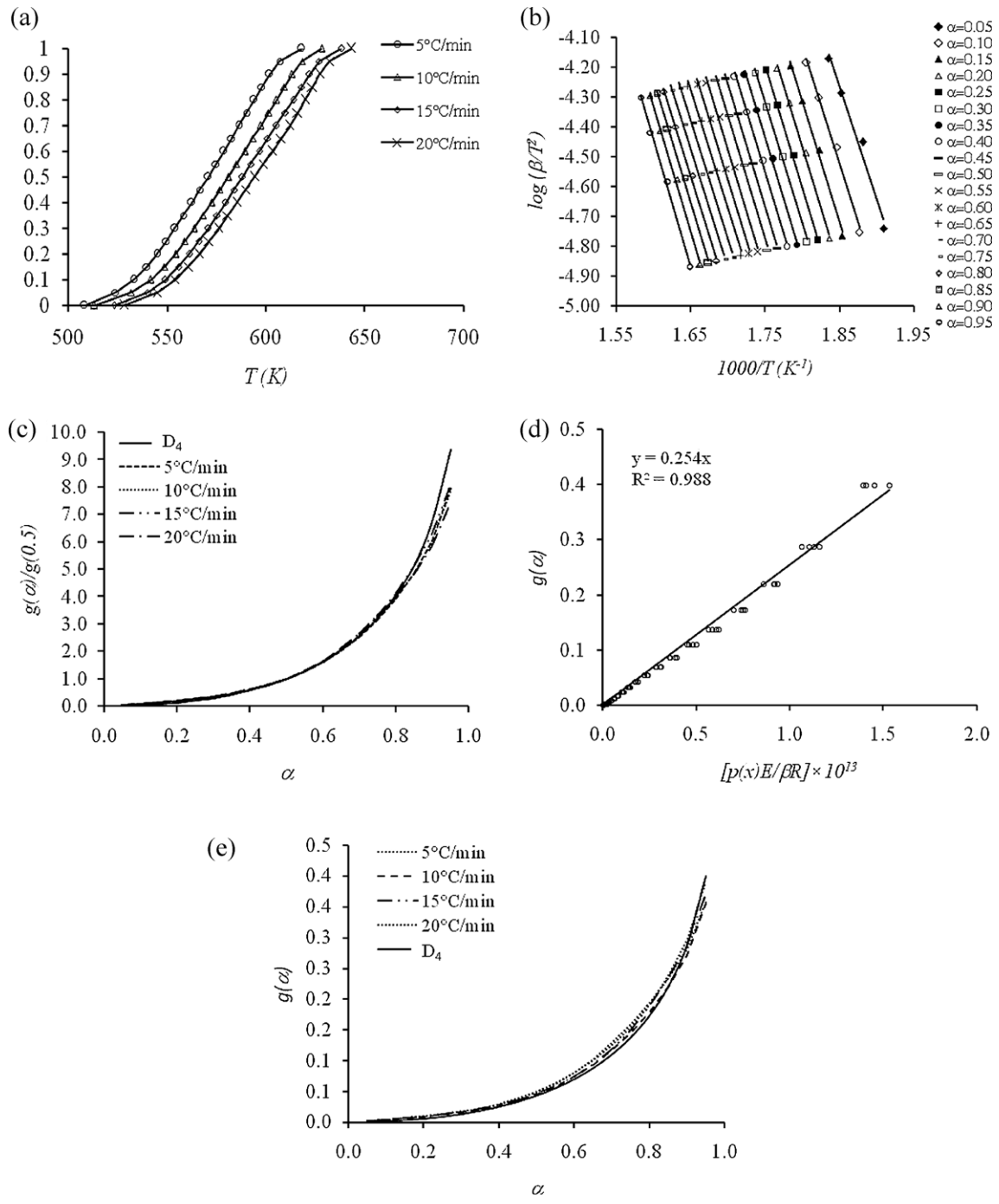

Fig. 6. Determination of kinetic model for OB degradation at stage II: (a) α–T curve, (b) KAS plot to calculate the activation energy, (c) experimental and theoretical master plots, (d) determination of A, (e) reconstructed $g(\alpha)$ model.

Table 2
Thermal parameters for polymers under study.

Sample code	Degradation stage	Temperature range (°C)	E (kJ mol^{-1})	ln$A$	Mechanism
PO	I	Ambient–115	51.58	–	Desorption
	II	215–310	118.15	24.09	$P_{3/2}$
	III	280–330	157.78	32.19	A_4
SA	I	Ambient–115	29.11	–	Desorption
	II	215–365	167.41	30.93	D_4
OB	I	Ambient–115	29.65	–	Desorption
	II	235–370	155.46	28.56	D_4

Please cite this article in press as: Akbar, J., et al. Kinetics and mechanism of thermal degradation of pentose- and hexose-based carbohydrate polymers. *Carbohydrate Polymers* (2012), http://dx.doi.org/10.1016/j.carbpol.2012.07.008

polymers (SA: 287.2 °C, 0.46; OB: 300.8 °C, 0.48). These polymers also possess sufficiently good life to use them in various applications (Fig. 2d). For the purpose of comparison, the lifetime of Methocel® K15M was also determined as shown in Fig. 2d; the polymers under investigation appear to be more stable. The DSC scans (Fig. 1b and c) showed that the stage I was endothermic and the stages II and III were exothermic as expected.

The similarity in the thermal behavior of these polymers reflects the similarity in their structures as reported in the literature (Azuma & Sakamoto, 2003; Chatterjee & Mukherjee, 1958). Both of these polymers are mainly composed of hexoses. On the other hand, the arabinoxylan from PO is mainly composed of pentoses (Saghir et al., 2008), therefore, its degradation mechanism was found to be quite different. However, the average E values at stage III for PO polymer and at stage II for SA and OB polymers are not significantly different (Table 2). Therefore, it may be concluded that the energy requirements for major degradation of the hexose- and pentose-based polymers under study are almost similar but they follow different decomposition mechanisms.

4. Conclusions

The kinetics and mechanism of thermal decomposition of carbohydrate polymers isolated from SA, OB and PO were studied by isoconversional method. The thermal decomposition behavior of SA and OB polymers, being hexose-based, was quite similar having comparable E and A values. Both of them followed D_4 mechanism for the single major degradation stage. The PO, being a pentose-based polymer, showed a distinct behavior by exhibiting a two-stage decomposition following the $P_{3/2}$ and A_4 mechanisms. The E values at different stages were considerably constant at different degrees of conversion suggesting single step degradation kinetics for the polymers. The polymers appear to be highly stable with longer lifetime as compared with some of the commercially important carbohydrate polymers such as Methocel® K15M. This study clearly shows that the hexose- and pentose-based polymers follow different decomposition mechanisms.

References

Aggarwal, P., Dollimore, D., & Heon, K. (1997). Comparative thermal analysis study of two biopolymers, starch and cellulose. *Journal of Thermal Analysis and Calorimetry*, *50*(1), 7–17.
Akbar, J., Iqbal, M. S., Chaudhary, M. T., Yasin, T., & Massey, S. (2012). A QSPR study of drug release from an arabinoxylan using ab initio optimization and neural networks. *Carbohydrate Polymers*, *88*(4), 1348–1357.
Azuma, J., & Sakamoto, M. (2003). Cellulosic hydrocolloid system present in seed of plants. *Trends in Glycoscience Glycotechnology*, *15*(81), 1–14.
Barbucci, R. (Ed.). (2009). *Hydrogels: Biological properties and applications*. Milan, Italia: Springer-Verlag.
Chatterjee, A. K., & Mukherjee, S. (1958). The structure of Tukhmalanga (*Salvia aegyptica*) mucilage. Part I. Nature of sugars present and the structure of the adobiouronic acid. *Journal of the American Chemical Society*, *80*(10), 2538–2540.
Chrissafis, K. (2009). Kinetics of thermal degradation of polymers. *Journal of Thermal Analysis and Calorimetry*, *95*(1), 273–283.
Fariba, G., & Ebrahim, V.-F. (2009). Hydrogels in controlled drug delivery systems. *Iranian Polymer Journal*, *18*(1), 63–88.
Fischer, M. H., Yu, N., Gray, G. R., Ralph, J., Anderson, L., & Marlett, J. A. (2004). The gel-forming polysaccharide of psyllium husk (*Plantago ovata* Forsk). *Carbohydrate Research*, *339*(11), 2009–2017.
Gupta, P., Vermani, K., & Garg, S. (2002). Hydrogels: From controlled release to pH-responsive drug delivery. *Drug Discovery Today*, *7*(10), 569–579.
Hoare, T. R., & Kohane, D. S. (2008). Hydrogels in drug delivery: Progress and challenges. *Polymer*, *49*(8), 1993–2007.
Hosseini-Parvar, S. H., Matia-Merino, L., Goh, K. K. T., Razavi, S. M. A., & Mortazavi, S. A. (2010). Steady shear flow behavior of gum extracted from *Ocimum basilicum* L. seed: Effect of concentration and temperature. *Journal of Food Engineering*, *101*(3), 236–243.
Iqbal, M. S., Akbar, J., Hussain, M. A., Saghir, S., & Sher, M. (2011). Evaluation of hot-water extracted arabinoxylans from ispaghula seeds as drug carriers. *Carbohydrate Polymers*, *83*(3), 1218–1225.
Iqbal, M. S., Akbar, J., Saghir, S., Karim, A., Koschella, A., Heinze, T., & Sher, M. (2011). Thermal studies of plant carbohydrate polymer hydrogels. *Carbohydrate Polymers*, *86*(4), 1775–1783.
Janković, B. (2008). Kinetic analysis of the nonisothermal decomposition of potassium metabisulfite using the model-fitting and isoconversional (model-free) methods. *Chemical Engineering Journal*, *139*(1), 128–135.
Laidlaw, R. A., & Purcival, E. G. V. (1949). Studies on seed mucilages. Part III. Examination of a polysaccharide extracted from the seeds of *Plantago ovata* Forsk. *Journal of the Chemical Society*, 1600–1607.
Laidlaw, R. A., & Purcival, E. G. V. (1950). Studies of seed mucilages. Part V. Examination of a polysaccharide extracted from the seeds of *Plantago ovata* Forsk by hot water. *Journal of the Chemical Society*, 528–534.
Prado, J. R., & Vyazovkin, S. (2011). Activation energies of water vaporization from the bulk and from laponite, montmorillonite, and chitosan powders. *Thermochimica Acta*, *524*(1–2), 197–201.
Ruel-Gariépy, E., & Leroux, J.-C. (2006). Chitosan: A natural polycation with multiple applications. In R. H. Marchessault, F. Ravenelle, & X. X. Zhu (Eds.), *Polysaccharides for drug delivery and pharmaceutical applications* (pp. 243–259). American Chemical Society.
Saghir, S., Iqbal, M. S., Hussain, M. A., Koschella, A., & Heinze, T. (2008). Structure characterization and carboxymethylation of arabinoxylan isolated from Ispaghula (*Plantago ovata*) seed husk. *Carbohydrate Polymers*, *74*(2), 309–317.
Senum, G. I., & Yang, R. T. (1977). Rational approximations of the integral of the Arrhenius function. *Journal of Thermal Analysis and Calorimetry*, *11*(3), 445–447.
Singh, B. (2007). Psyllium as therapeutic and drug delivery agent. *International Journal of Pharmaceutics*, *334*(1–2), 1–14.
Turmanova, S. C., Genieva, S. D., Dimitrova, A. S., & Vlaev, L. T. (2008). Non-isothermal degradation kinetics of filled with rise husk ash polypropene composites. *Express Polymer Letters*, *2*(2), 133–146.
Villetti, M. A., Crespo, J. S., Soldi, M. S., Pires, A. T. N., Borsali, R., & Soldi, V. (2002). Thermal degradation of natural polymers. *Journal of Thermal Analysis and Calorimetry*, *67*(2), 295–303.
Vyazovkin, S., Burnham, A. K., Criado, J. M., Pérez-Maqueda, L. A., Popescu, C., & Sbirrazzuoli, N. (2011). ICTAC kinetics committee recommendations for performing kinetic computations on thermal analysis data. *Thermochimica Acta*, *520*(1–2), 1–19.
Yang, H., Yan, R., Chen, H., Lee, D. H., & Zheng, C. (2007). Characteristics of hemicellulose, cellulose and lignin pyrolysis. *Fuel*, *86*(12–13), 1781–1788.
Zohuriaan, M. J., & Shokrolahi, F. (2004). Thermal studies on natural and modified gums. *Polymer Testing*, *23*(5), 575–579.

Please cite this article in press as: Akbar, J., et al. Kinetics and mechanism of thermal degradation of pentose- and hexose-based carbohydrate polymers. *Carbohydrate Polymers* (2012), http://dx.doi.org/10.1016/j.carbpol.2012.07.008